International Journal of Computational and Experimental Science and ENgineering (IJCESEN)

Vol. 12-No.3 (2026) pp.1-7
http://www.ijcesen.com

ISSN: 2149-9144

Research Article

Influence Of Inclined-End Baffle Orientation On The Thermal And Thermodynamic Performance Of A Rectangular Channel: A Numerical Investigation

Djemaa Belakhal[1*], Khadra Houari[2], Amar Kouadri[3], Embarek Douroum[4,5], Soumia Bouakkaz[6], Zehor Allam[7]

[1]Laboratory for Inorganic, Organic and Bio-Inspired Chemistry Research, University of Djelfa 17000, Algeria.
* **Corresponding Author Email:** d.belakhal@univ-djelfa.dz- **ORCID:** 0009-0004-0696-3171

[2] Department of mechanical, Faculty of technology, University of Djelfa, 17000. Algeria.
Email: khadra.haouari@univ-djelfa.dz - **ORCID:** 0009-0009-4317-5066

[3] Renewable Energy Systems Applications Laboratory, LASER, University of Djelfa 17000, Algeria.
Email: amar.kouadri@univ-djelfa.dz - **ORCID:** 0000-0001-5572-811X

[4]Laboratory of materials and reactive systems, LMSR, Djillali Liabes University, Sidi Bel Abbes 22000, Algeria.
[5] Renewable Energy Systems Applications Laboratory, LASER, University of Djelfa 17000, Algeria.
Email: embarek.douroum@univ-djelfa.dz - **ORCID:** 0000-0001-6664-8414

[6] Department of Chemistry, Faculty of Exact Sciences and Computer Science, University of Djelfa, 17000. Algeria
Email: s.bouakkaz@univ-djelfa.dz - **ORCID:** 0009-0005-2525-188X

[7] Department of Physics, Faculty of Exact Sciences and Computer Science,17000, Djelfa. Algeria
Email: z.allam@univ-djelfa.dz- **ORCID:** 0009-0006-2249-7398

Article Info:

DOI: 10.22399/ijcesen.5310
Received: 12 December 2025
Revised: 10 May 2026
Accepted: 20 May 2026

Keywords

Inclined-end baffles
Heat exchanger
Reynolds number
Bejan number

Abstract:

A numerical study was conducted to investigate the influence of inclined-end baffle orientation on the thermal and thermodynamic performance of a rectangular channel equipped with two baffles. Four geometric configurations were examined while maintaining the same inclination angle (45°) and varying only the baffle orientation. The analysis was performed using Computational Fluid Dynamics (CFD) in ANSYS Fluent, based on the Finite Volume Method (FVM) and the SIMPLE algorithm, with the standard k-ε turbulence model. The study evaluated velocity, pressure, and temperature fields, as well as the average Nusselt number, entropy generation, and Bejan number. The results showed that baffle orientation strongly affects flow behavior and heat transfer characteristics. The converging configuration provided the highest heat transfer performance with relatively low entropy generation, whereas the both-facing-downstream configuration yielded the lowest total entropy generation and the best thermodynamic performance.

1. Introduction

Over the past two decades, numerous strategies have been proposed to enhance heat transfer and flow dynamics in channels and heat exchangers. Early experimental and numerical work by Demartini et al [1] analyzed flow in baffle-equipped rectangular channels, revealing high-pressure regions upstream and recirculation zones downstream. Building on this, Menni et al [2,3] conducted multiple CFD studies on rectangular channels with staggered baffles, V-shaped and flat fins, and circular-rectangular turbulators (CRTBs). These studies demonstrated that such obstacles significantly intensify turbulent mixing and increase Nusselt numbers, although at the cost of higher friction factors and pressure drops. They further explored S-shaped, Z-shaped, and arc-downstream baffles, as well as cascaded deflectors highlighting how obstacle geometry, spacing, and orientation control recirculation zones, vortices, and local heat transfer [4,5]. Optimal designs produced substantial thermal enhancement factors (TEF).

Parallel studies by Menni et al [6] and Saha et al [7] emphasized the benefits of trapezoidal, plane, and S-shaped baffles in improving flow patterns and Nusselt numbers across varying Reynolds numbers, while maintaining manageable friction increases [7,8] and expanded this understanding by incorporating perforated and inclined baffles, as well as rectangular and triangular vortex generators (VGs). Their results showed that modifying geometry and orientation enhances turbulence and axial velocity, with triangular VGs and perforated designs offering the best synergy between mixing and pressure management.

Complementary research by Alqahtani et al [9] and Costa et al [10] employed porous baffles and gradient-porous ribs with nanofluids to balance heat transfer and pressure drop. These studies highlighted the critical role of permeability, rib porosity, and nanoparticle fraction in optimizing energy efficiency. More recently, studies on trapezoidal grooves and fin arrangements [11] as well as diamond-shaped obstacles in rectangular heat exchangers. Ghoulam et al [12] have shown that combined geometrical and fin modifications can maximize outlet temperatures and thermal performance in compact, high-efficiency systems.

Entropy generation analysis has emerged as an effective tool for evaluating heat exchanger performance by quantifying thermodynamic irreversibility's associated with heat transfer and fluid friction. Recent studies indicate that combining first-law indicators (Nusselt number and TEF) with second-law parameters (entropy generation and Bejan number) provides a more comprehensive thermo-hydraulic assessment[13, 14]. In this context, Thanh et al [15] numerically investigated a baffled cooling channel and reported that higher Reynolds numbers and larger baffle angles enhance heat transfer while reducing entropy generation, with Reynolds number identified as the most influential parameter.

The present work numerically investigates a rectangular channel fitted with two inclined-end baffles. Four different geometric configurations (varying only the orientation of the baffles while keeping their inclination angles identical) are proposed and analyzed. The study aims to identify the optimal configuration that provides the best compromise between heat transfer enhancement and entropy generation minimization, thereby improving the overall thermo-hydraulic performance of the system.

2. Mathematical Modeling

2.1 Geometry of the Rectangular Channel with Inclined-End Baffles

The present numerical configuration is based on a two-dimensional horizontal channel model representing a rectangular cross-section duct. The channel has a total length of L=0.554 m, a height of H=0.146 m constant temperature boundary condition T_w=375 K, while the lower wall is assumed to be thermally insulated. These geometric dimensions are adopted from the experimental and numerical investigation by Demartini et al [1] ensuring a reliable basis for validation and comparison.

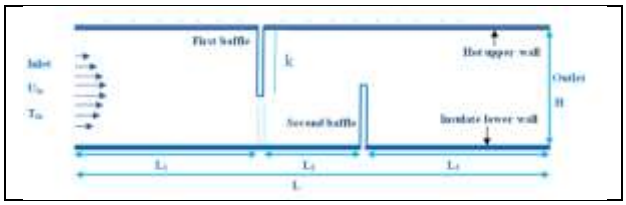

Figure1. *Rectangular channel with two straight baffles used for model validation [1]*

Within the channel, two baffles are placed alternately along the upper and lower walls in a staggered arrangement to generate vortical structures, enhance fluid mixing, and consequently improve heat transfer performance. The first baffle is positioned on the heated upper wall at a streamwise distance L_1=0.218 m from the inlet. The second baffle is located on the lower adiabatic wall at a distance L_3=0.174 m from the outlet. The baffle thickness is e=0.01 m, baffle length K=2h=0.08m, baffle length (S= h sinα=h sinβ) and the spacing between the two baffles is L_2=0.142 m.

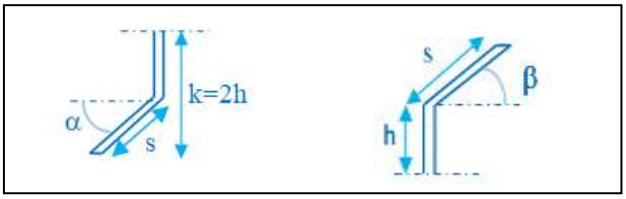

Figure2. *Schematic of the inclined baffles and, their geometric parameters*

The term "inclined-end baffle" means that the free tip of each baffle is cut at an angle relative to the wall normal, creating an inclined surface that directs flow. In all four configurations, the inclination angles of the two baffles are kept identical (α=β=45°), and only their orientation (e.g., both facing upstream, both facing downstream, converging, or diverging) is modified. This approach allows systematic analysis of the influence of baffle orientation on flow patterns, vortex formation, heat transfer, pressure losses, and entropy generation under identical geometric and

operating conditions. (Figure3 would show the four configurations schematically.)

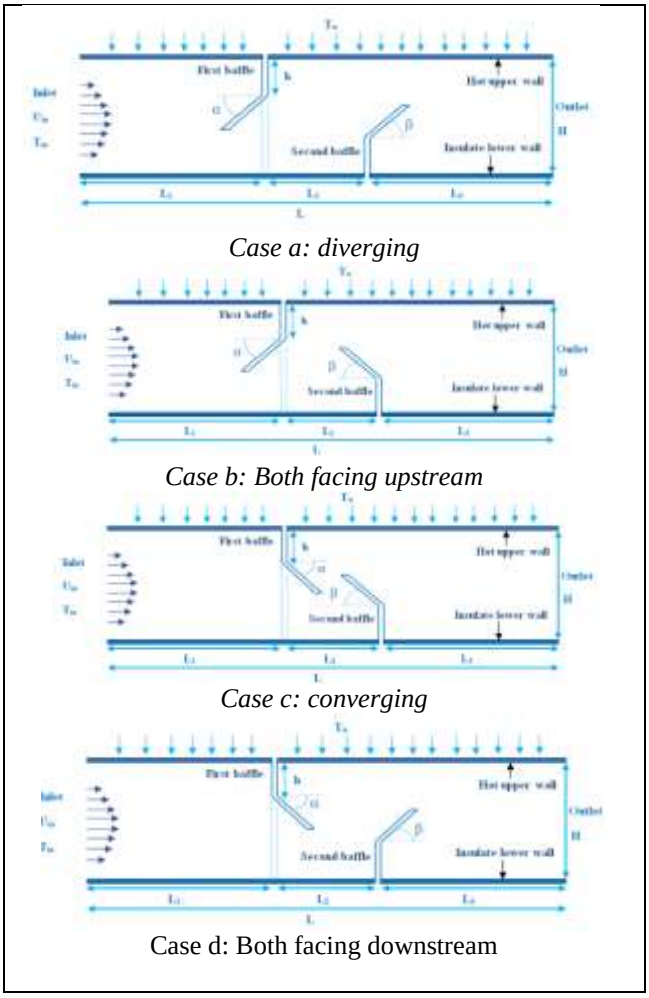

Case a: diverging

Case b: Both facing upstream

Case c: converging

Case d: Both facing downstream

Figure 3. *Geometrical configurations of the rectangular channel with two inclined-end baffles (Cases a–d)*

2.2 Physical Model and Governing Equations

The flow is assumed steady, incompressible, and turbulent. Air is considered a Newtonian fluid with constant thermo physical properties evaluated at the bulk mean temperature. Turbulence is modeled using the standard k-ε model with wall functions.

2.2.1 Governing Equations

The mathematical formulation of the present problem is based on the fundamental conservation of continuity (1), momentum (2), and energy (3). These governing equations describe the fluid flow and heat transfer phenomena occurring within the computational domain and can be expressed as follows:

$$\nabla \cdot \vec{V} = 0 \tag{1}$$

$$\rho(\vec{V} \cdot \nabla)\vec{V} = -\nabla P + \mu_f \nabla^2 \vec{V} \tag{2}$$

$$\rho c_p(\vec{V} \cdot \nabla T) = k_f \nabla^2 T \tag{3}$$

The standard k-ε model is defined by two transport equations, one for the turbulent kinetic energy, k and the other for its dissipation rate ε, as given below

$$\frac{\partial}{\partial x_i}(\rho k u_i) = \frac{\partial}{\partial x_j}\left[\left(\mu + \frac{\mu_t}{\sigma_k}\right)\frac{\partial k}{\partial x_j}\right] + G_k - \rho\varepsilon \tag{4}$$

$$\frac{\partial}{\partial x_i}(\rho\varepsilon u_i) = \frac{\partial}{\partial x_j}\left[\left(\mu + \frac{\mu_t}{\sigma_\varepsilon}\right)\frac{\partial \varepsilon}{\partial x_j}\right] + C_{1\varepsilon}\frac{\varepsilon}{k}G_k - C_{2\varepsilon}\rho\frac{\varepsilon^2}{k} \tag{5}$$

$$G_k = \mu_t\left(\frac{\partial u_i}{\partial x_j} + \frac{\partial u_j}{\partial x_i}\right)\frac{\partial u_i}{\partial x_j} \tag{6}$$

The turbulent viscosity, μt is modeled as follows:

$$\mu_t = \rho C_\mu \frac{k^2}{\varepsilon} \tag{7}$$

In these equations, G_k represents the generation of turbulence kinetic energy due to the mean velocity gradients. The related constant parameters are.

$$C_{1\varepsilon} = 1.44, \quad C_{2\varepsilon} = 1.92, \quad C_\mu = 0.09, \quad \sigma_k = 1.0, \quad \sigma_\varepsilon = 1.3 \tag{8}$$

The Reynolds number is defined as

$$Re = \frac{\rho U D_h}{\mu} \tag{9}$$

The local Nusselt number, Nu_x which can be written as

$$Nu_x = \frac{h_x D_h}{\lambda_f} \tag{10}$$

The average Nusselt number, *Nu* can be obtained by

$$Nu_{av} = \frac{1}{L}\int Nu_x \, dx \tag{11}$$

Where, h_x: is the local convective heat transfer coefficient.

2.2.2. Entropy generation rate

$$S_{total} = S_{thermal} + S_{frictional} \tag{12}$$

Where :

$$S_{thermal} = \frac{\lambda_{eff}}{T^2}\left[\left(\frac{\partial T}{\partial x}\right)^2 + \left(\frac{\partial T}{\partial y}\right)^2\right] \tag{13}$$

$$S_{frictional} = \frac{1}{2}\left(\frac{\mu_{eff}}{T}\right)\left[\left(\frac{\partial u}{\partial x}\right)^2 + \left(\frac{\partial v}{\partial y}\right)^2 + 2\left(\frac{\partial u}{\partial y} + \frac{\partial v}{\partial x}\right)^2\right] \tag{14}$$

Here λ and μ are, respectively, the thermal conductivity and the dynamic viscosity of the fluid. The terms u, v, w and T denote the components of the fluid velocity and the fluid's temperature. Also, $S_{thermal}$is the entropy generation resulting from heat transfer and $S_{frictional}$ also, accounts for the entropy generation due to fluid friction [16].

2.2.3. Bejan number:

$$Be = \frac{\dot{S}_{thermal}}{\dot{S}_{thermal} + \dot{S}_{frictional}} \quad (15)$$

2.2.4 Boundary Conditions

a. Inlet: Uniform velocity u_{in} corresponding to the desired Reynolds number, with constant inlet temperature T_{in}=300 K, and turbulence intensity I=5%.
b. Outlet: Pressure outlet (gauge pressure = 0 Pa).
c. Upper wall: No-slip, constant temperature Tw=375 K.
d. Lower wall: No-slip, adiabatic ($\partial T/\partial n=0$).
e. Baffle surfaces: No-slip, adiabatic.

3. Numerical model and Mesh generation analysis

3.1. Numerical model

The governing equations were solved using the finite volume method with the SIMPLE algorithm for pressure–velocity coupling. Turbulence was modelled using the standard k-ε model, and all computations were performed in ANSYS Fluent.

3.2. Mesh sensitivity analysis

A grid independence study was conducted to ensure the accuracy and reliability of the numerical results. Six different mesh densities, ranging from 20,000 to 145,000 elements, were tested, and the corresponding average Nusselt numbers were evaluated.
As shown in Figure 4, the average Nusselt number increased with mesh refinement and became nearly constant beyond 94,322 elements, indicating mesh-independent results. Therefore, the mesh containing 94,322 elements was selected for all simulations, ensuring accurate results with reasonable computational cost. The comparison shows a good agreement between the two sets of results, with the present numerical predictions closely following the experimental trend. This satisfactory concordance confirms the accuracy and reliability of the numerical model adopted in the present study.

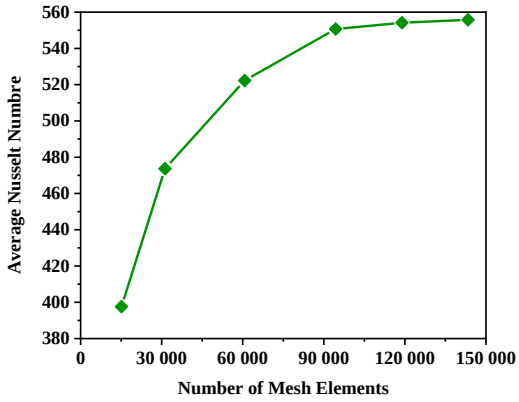

Figure 4. *Grid independence study*

4. Results and discussion

4.1. CFD code validation

Figure 5 compares the axial velocity profiles obtained from the present CFD simulation with the experimental data [1] at x=0.525 m.

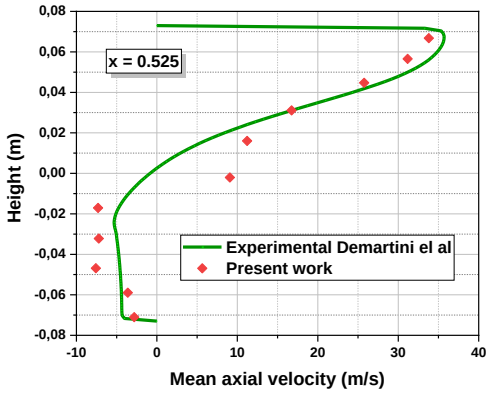

Figure 5. *Axial velocity profile validation*

Figure6, illustrates the velocity magnitude distributions for the four channel configurations. In all cases, the flow accelerates through the narrowed section due to the reduction in flow area, while low-velocity recirculation zones develop near the walls and downstream of the inclined surfaces [1, 4]. The wall orientation significantly affects the flow structure: the both-facing-downstream configuration produces the smoothest and most uniform velocity field, whereas the diverging arrangement generates stronger acceleration, larger recirculation regions, and enhanced mixing. These secondary flow structures improve convective heat transfer but may also increase pressure losses. Overall, the both-facing-downstream case offers the most stable flow behavior, while the diverging case provides the strongest flow enhancement.

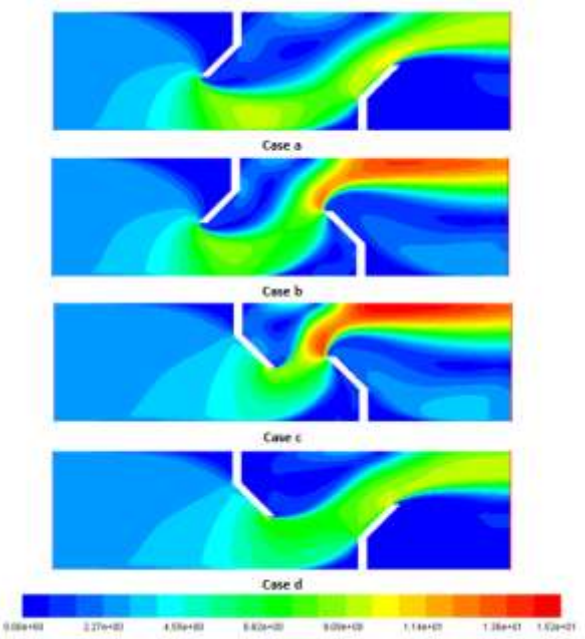

Figure 6.*Velocity magnitude contours for the investigated channel configurations.*

Figure 7.Shows the static pressure distributions for the four channel configurations. In all cases, high-pressure regions develop upstream of the constricted section, followed by a pressure decrease as the flow accelerates through the reduced area.
inclined walls due to flow separation and recirculation[4]. The both-facing-downstream configuration exhibits smoother pressure variations and lower flow disturbances, while the converging and diverging arrangements promote stronger acceleration and recirculation, leading to larger pressure losses.

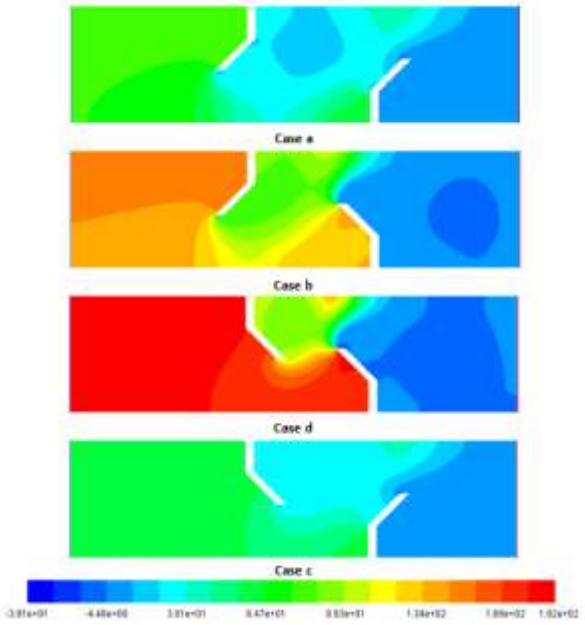

Figure7.*Static pressure contours for the investigated channel configurations*

Low-pressure zones appear downstream of the Overall, the pressure field is strongly influenced by the orientation of the inclined walls and the resulting flow structure[1,4].
Figure8, shows the temperature distributions for the both-facing-upstream, both-facing-downstream, converging, and diverging configurations. The temperature field is strongly influenced by the flow structures generated inside the channel. Recirculation zones enhance fluid mixing between the heated wall regions and the core flow, leading to improved heat transfer [8, 9].The both-facing-upstream configuration produces a relatively uniform temperature field, while the converging and diverging arrangements promote stronger mixing and larger temperature gradients. [8,9,15]

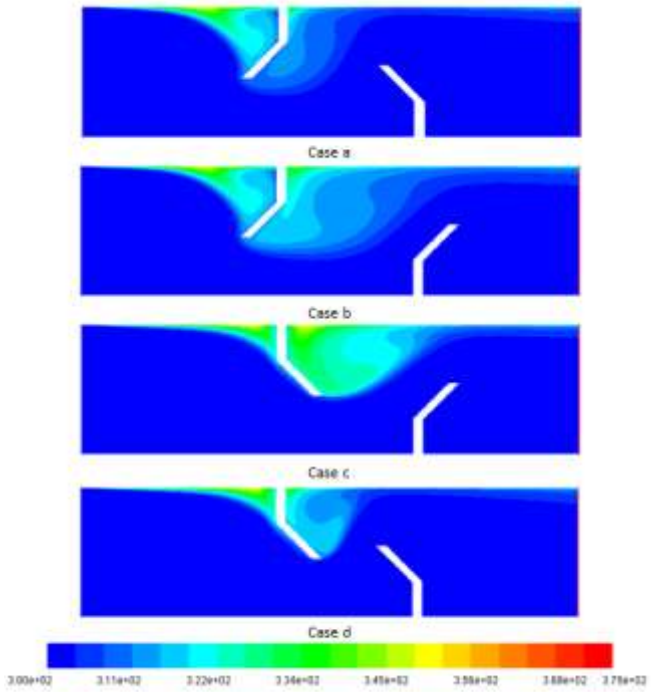

Figure 8.*Temperature contours for the investigated channel configurations*

The both-facing-downstream configuration provides a more homogeneous temperature distribution and efficient thermal transport. Consequently, enhanced convective heat transfer is achieved for the configurations that generate stronger mixing effects.
Table 2 presents the total entropy generation (S_{total}), heat transfer entropy generation ($S_{thermal}$), fluid friction entropy generation ($S_{frictional}$), average Nusselt number (Nu_{av}) , and

Table 1. *Entropy Generation Analysis and Heat Transfer Performance for Different Cases*

	S_{total} (w/k)	$S_{thermal}$(w/k)	$S_{frictional}$(w/k)	Be	Nu_{av}
Case a	1098.7999	1094.216	4.5838974	0.9958	487.87486
Case b	799.35769	794.29768	13.46426	0.9937	549.83627
Case c	778.82609	773.02539	5.8007038	0.9926	584.71071
Case d	659.08454	656.80856	2.2759841	0.9965	382.01223

Bejan number (Be) for the investigated cases. The results reveal noticeable variations in both thermodynamic losses and heat transfer performance among the different configurations. For all cases, The Bejan number remains very close to unity (Be > 0.99) for all cases, confirming that heat transfer irreversibility dominates entropy generation, while fluid friction contributes negligibly [13, 14,16] .

- Case a shows the highest total entropy generation (1098.80w/k) with moderate heat transfer (Nu_{av} = 487.87).
- Case b reduces entropy generation to 799.36 w/k and improves heat transfer (Nu_{av}= 549.84), but exhibits the highest frictional entropy (13.46 w/k) and lowest Be (0.9937), indicating more pronounced viscous effects.
- Case c achieves the best heat transfer performance (Nu_{av} = 584.71) while maintaining relatively low entropy generation (778.83w/k).
- Case d minimizes total entropy generation (659.08w/k) and maximizes Be (0.9965), but at the expense of heat transfer (Nu_{av} = 382.01).

In conclusion, thermal irreversibility governs all configurations. Case c is optimal for heat transfer enhancement, whereas case d is best for entropy minimization. A clear trade-off exists between maximizing heat transfer and reducing thermodynamic losses.

5. Conclusion

- A two-dimensional CFD analysis was performed to investigate the effect of inclined-end baffle orientation on the thermal and thermodynamic behavior of a rectangular channel under turbulent airflow conditions.
- Four configurations were examined:
  - Case a: Diverging arrangement.
  - Case b: Both baffles facing upstream.
  - Case c: Converging arrangement.
  - Case d: Both baffles facing downstream
- Baffle orientation was found to have a significant impact on flow structure, heat transfer, and entropy generation.
- For all configurations, the Bejan number exceeded 0.99, indicating that thermal irreversibility dominates, whereas frictional irreversibility remains negligible.
- Case a (diverging) produced the highest total entropy generation.
- Case b (both-facing-upstream) exhibited the largest frictional entropy generation due to stronger viscous effects.
- Case c (converging) achieved the highest average Nusselt number with relatively low entropy generation, making it the most effective configuration for heat transfer enhancement.
- Case d (both-facing-downstream) yielded the lowest total entropy generation and the highest Bejan number, corresponding to the best thermodynamic performance but lower heat transfer capability.
- A clear trade-off exists between maximizing heat transfer and minimizing irreversibilities.
- The results demonstrate that inclined-end baffle orientation is a key parameter for optimizing baffled channel performance.
- Future studies should include a comprehensive thermo-hydraulic evaluation based on both first-law and second-law criteria to determine the optimum configuration.

Author Statements:

- **Ethical approval:** The conducted research is not related to either human or animal use.
- **Conflict of interest:** The authors declare that they have no known competing financial interests or personal relationships that could have appeared to influence the work reported in this paper
- **Acknowledgement:** The authors declare that they have nobody or no-company to acknowledge.

References

[1] L. C. Demartini, H. A. Vielmo, and S. Möller, "Numeric and experimental analysis of the turbulent flow through a channel with baffle plates," *Journal of the Brazilian Society of Mechanical Sciences and Engineering*, vol. 26, pp. 153–159, 2004.

[2] Y. Menni, A. Azzi, and C. Zidani, "Use of waisted triangular-shaped baffles to enhance heat transfer in

a constant temperature-surfaced rectangular channel," *Journal of Engineering Science and Technology*, vol. 12, no. 12, pp. 3251–3273, 2017.

[3] Y. Menni, A. Azzi, and A. Chamkha, "Optimal thermo aerodynamic performance of s-shaped baffled channels," *Journal of Mechanical Engineering and Sciences*, vol. 12, no. 3, pp. 3888–3913, 2018.

[4] Y. Menni, A. Azzi, A. J. Chamkha, and S. Harmand, "Effect of wall-mounted V-baffle position in a turbulent flow through a channel: Analysis of best configuration for optimal heat transfer," *International Journal of Numerical Methods for Heat & Fluid Flow*, vol. 29, no. 10, pp. 3908–3937, 2019.

[5] Y. Menni, A. J. Chamkha, and O. D. Makinde, "Turbulent heat transfer characteristics of a W-baffled channel flow-heat transfer aspect," presented at the Defect and diffusion forum, Trans Tech Publ, 2020, pp. 117–130.

[6] Y. Menni *et al.*, "Enhancement of the turbulent convective heat transfer in channels through the baffling technique and oil/multiwalled carbon nanotube nanofluids," *Numerical Heat Transfer, Part A: Applications*, vol. 79, no. 4, pp. 311–351, 2020.

[7] S. Saha, "Numerical simulation of turbulent airflow and heat transfer through a rectangular channel along with two trapezoidal baffle plates: Comparison between plane and trapezoidal shape baffles," presented at the AIP Conference Proceedings, AIP Publishing LLC, 2021, p. 030005.

[8] K. Mahdi *et al.*, "Using obstacle perforation, reconfiguration, and inclination techniques to enhance the dynamic and thermal structure of a top-entry channel," *Thermal Science*, vol. 26, no. Spec. issue 1, pp. 475–484, 2022.

[9] S. Alqahtani *et al.*, "Enhancing flow structure in heat exchangers analysis of dynamic and thermal air-flow behavior with perforated and inclined baffles," *Thermal Science*, vol. 27, no. 4 Part B, pp. 3269–3280, 2023.

[10] S. C. Costa, F. M. Janeiro, and I. Malico, "Multi-objective optimisation of a 2D backward-sfacing step channel with porous baffles," *Journal of Thermal Analysis and Calorimetry*, vol. 149, no. 10, pp. 4755–4770, 2024.

[11] H.-R. Bahrami and M. Ghaedi, "Using a Nonuniform Magnetic Field to Enhance Heat Transfer before a Sudden Compression in a 2D Milli-Channel," *Journal of Enhanced Heat Transfer*, vol. 31, no. 4, 2024.

[12] O. Ghoulam, H. Talbi, K. Amghar, A. Amrani, A. Charef, and I. Driouch, "Heat transfer improvement in turbulent flow using detached obstacles in heat exchanger duct," *International Journal of thermofluids*, vol. 27, p. 101225, 2025.

[13] A. Kaood, A. Aboulmagd, and A. ElDegwy, "Entropy generation analysis of turbulent flow in conical tubes with dimples: a numerical study," *Journal of Thermal Analysis and Calorimetry*, vol. 148, no. 12, pp. 5667–5685, 2023.

[14] P. B. Jasiński, G. Górecki, and Z. Cebulski, "Evaluation of the Efficiency of Heat Exchanger Channels with Different Flow Turbulence Methods Using the Entropy Generation Minimization Criterion," *Energies*, vol. 18, no. 1, p. 132, 2024.

[15] L. N. Thanh, "The influence of baffled channel for cooling hot surface: Numerical simulation and Taguchi analysis," *Case Studies in Thermal Engineering*, vol. 52, p. 103646, 2023.

[16] D. Belakhal, K. Rahmani, A. E. Elkaroui, S. B. H. Ayech, N. M. Saïd, and B. Imine, "Numerical study of asymmetric and axisymmetric thermal jet with entropy generation concept," *Journal of Mechanical Engineering and Sciences*, vol. 15, no. 1, pp. 7628–7636, 2021.